




Article

Drought Risk Analysis in the Eastern Cape Province of South Africa: The Copula Lens

Christina M. Botai ^{1,*}, Joel O. Botai ^{1,2,3}, Abiodun M. Adeola ^{1,4}, Jaco P. de Wit ¹,
Katlego P. Ncongwane ^{1,5} and Nosipho N. Zwane ¹

¹ South African Weather Service, Private Bag X097, Pretoria 0001, South Africa;

Joel.Botai@weathersa.co.za (J.O.B.); Abiodun.Adeola@weathersa.co.za (A.M.A.);

Jaco.deWit@weathersa.co.za (J.P.d.W.); Katlego.Ncongwane@weathersa.co.za (K.P.N.);

Nosipho.Zwane@weathersa.co.za (N.N.Z.)

² Department of Geography, Geoinformatics and Meteorology, University of Pretoria, Private Bag X020, Hatfield 0028, South Africa

³ Department of Information Technology, Central University of Technology, Bloemfontein 9301, South Africa

⁴ Institute for Sustainable Malaria Control, University of Pretoria, Pretoria 0002, South Africa

⁵ School of Geography and Environmental Science, University of KwaZulu-Natal, Durban 4041, South Africa

* Correspondence: Christina.Botai@weathersa.co.za; Tel.: +27-12-367-6269

Received: 28 May 2020; Accepted: 3 July 2020; Published: 8 July 2020



Abstract: This research study was carried out to investigate the characteristics of drought based on the joint distribution of two dependent variables, the duration and severity, in the Eastern Cape Province, South Africa. The drought variables were computed from the Standardized Precipitation Index for 6- and 12-month accumulation period (hereafter SPI-6 and SPI-12) time series calculated from the monthly rainfall data spanning the last five decades. In this context, the characteristics of climatological drought duration and severity were based on multivariate copula analysis. Five copula functions (from the Archimedean and Elliptical families) were selected and fitted to the drought duration and severity series in order to assess the dependency measure of the two variables. In addition, Joe and Gaussian copula functions were considered and fitted to the drought duration and severity to assess the joint return periods for the dual and cooperative cases. The results indicate that the dependency measure of drought duration and severity are best described by Tawn copula families. The dependence structure results suggest that the study area exhibited low probability of drought duration and high probability of drought severity. Furthermore, the multivariate return period for the dual case is found to be always longer across all the selected univariate return periods. Based on multivariate analysis, the study area (particularly Buffalo City, OR Tambo and Alfred Zoo regions) is determined to have higher/lower risks in terms of the conjunctive/cooperative multivariate drought risk (copula) probability index. The results of the present study could contribute towards policy and decision making through e.g., formulation of the forward-looking contingent plans for sustainable management of water resources and the consequent applications in the preparedness for and adaptation to the drought risks in the water-linked sectors of the economy.

Keywords: drought; dependence measure; Standardized Precipitation Index; copula; return periods

1. Introduction

The synchronous anomalous climatic conditions that society experiences today did not return; it never went away. This is especially true because the theme about mankind's struggle with climatic adversaries has always been interwoven in the world's stock of e.g., documentary, religion and mythology literature. In this regard, drought conditions are the most profound and omnipresent

adverse weather phenomena that manifests as an extended period of deficit precipitation relative to normal [1,2]. As a corollary, drought exhibits a global footprint mimicking the spatial–temporal nature of variability of precipitation. From the temporal viewpoint, drought conditions manifesting as insufficient or delayed precipitation is classified as a meteorological drought [1], with the definition relating to the imbalance of water availability with in-consistence to persistent lower than average precipitation [2]. The condition that relates to insufficient soil moisture is classified as an agricultural drought, with the impacts manifested from crop failure, leading to a treat in food security [3]. On the other hand, a hydrological drought describes a condition whereby water availability in water reservoirs is significantly below normal levels over a specific period, a condition attributed to low precipitation coupled with increased evapotranspiration rates, thereby threatening water security [4]. In general, the inherent impacts of drought are naturally complex and often resonate across social, environmental, and economic sectors, including water, agriculture, energy, health, tourism, etc. [5]. There is compelling evidence that drought is the most damaging and pressing natural disaster with the highest frequency, the most critical disaster with significant socio-economic and ecological losses as well as the most commodious impact [6,7], causing significant damage in infrastructure and property as well as well loss of life in general [8]. There is, therefore, a need to monitor and evaluate drought events, from global to regional timescales, so to alleviate the impacts and for preparedness measures for future events.

Drought indices are traditionally used for drought assessment, monitoring, and prediction. Such indices have been developed based on various datasets types e.g., precipitation only (the Standardized Precipitation Index (SPI); [9]), streamflow only (the Standardized Streamflow Index (SSI); [10]) as well as those derived from a combination of hydro-meteorological parameters, such as precipitation and temperature (the Standardized Precipitation and Evapotranspiration Index (SPEI); [11]), and precipitation, temperature and streamflow (Palmer Modified Drought Index (PDSI); [12]). Most of these indices have been evaluated and confirmed to be appropriate tools for monitoring, assessment (features such as the onset, the intensity, severity and frequency) as well as prediction of drought [13]. The SPI, particularly, has been extensively used for drought assessment, across the world, for instance in South Africa [13–16], in Bangladesh [17,18], India [19], and China [20]. Drought analysis and monitoring has also been conducted based on SPEI, for examples see studies by [13,21,22] and references therein.

Previous research studies on drought over South Africa have alluded to the occurrence of widespread and persistent drying conditions in most parts of the country [13–16,23]. Five of the most economically important/driven provinces of South Africa are recently recovering from severe drought, which caused negative socio-economic impacts, including the disruption of water supply and agricultural activities. These conditions have resulted in a significantly high cost of living, particularly to the most vulnerable communities, including farmers that mostly depend on rain-fed agriculture. The projected increases in the frequency of climate-related extremes, including drought disasters [24,25], pose a significant threat to South Africa given the vulnerability of the country, e.g., more than 90% of the country is arid to semi-arid [26]. Well-deserved attention needs to be given to drought features such as the duration, frequency, and severity, including the potential increase of drought disaster in general. Furthermore, effective measures of dealing with future drought and its inherent impacts are needed, so as to help inform the design of programs to reduce, mitigate, and prepare for future drought related impacts.

Multivariate distribution methods, based on copulas, are often used to evaluate and model drought features, such as the onset, duration, frequency, intensity, and severity [27,28]. For example, studies by [27] used two-dimensional copula functions to model the joint drought duration and severity distribution by fitting exponential and gamma distribution functions to the drought features, respectively. In [29], copulas were used to construct and investigate hydrological droughts of the Yellow River in northern China. A study in Iran used a copula-based distribution function to model the joint distribution of drought duration and severity for the period of 1954–2003 [30]. In addition, [31] applied trivariate copulas on the SPI series and characterized drought events under

El-Nino, La-Nina, and natural states. Similarly, using trivariate copulas, [32] evaluated the joint behaviour of drought characteristics (e.g., duration, severity, and intensity) under changing climate in Oregon's upper Klamath River basin. Furthermore, [33] evaluated the influence of the tail shape of various copula functions on drought bivariate frequency analysis. Several copulas from Archimedean and meta-elliptical families were used by [34] to model four-dimensional joint distributions on the SPI and evaluate drought characteristics such as drought duration, severity and interval time.

In South Africa, the SPI drought index has been used to study drought characteristics at different timescales [13,15,16,34–37] at national and regional level. Studies by [13,15] focused on drought characteristics in the Free State and North West as well as in the Western Cape provinces, respectively. Owing to the economic value of drought impacts in South Africa, the literature on drought monitoring and prediction from the viewpoint of drought indicators has continued to grow. A salient feature in all these studies is the quantification of drought conditions using univariate methods. Unlike multivariate-based risk assessment, the univariate quantification of droughts are not duly suited for estimating the true impacts of droughts.

In general, the use of multivariate copula functions to study drought characteristics has been widely supported in the literature. Research studies on drought characteristics based on multivariate copula-based distribution approaches have been rarely reported in South Africa, although such methods offer an improved alternative approach to study the joint distribution of drought characteristics, such as duration, severity, frequency, and intensity, as well as the minimum SPI values within specific drought period.

In this regard, the joint distribution analysis of the drought duration, severity, and frequency can provide essential information regarding the historical drought events and such information could be used in water resources management and planning. For this purpose, the current research study is focused on utilizing the multivariate copula-based functions to analyze characteristics of the joint distribution of drought duration and severity in the Eastern Cape province of South Africa. The characteristics of the joint distribution of drought duration and severity is derived from the SPI time series computed from monthly rainfall observational data. The results of this research work contribute towards drought monitoring for effective water resources management and planning. This paper is structured as follows: first, a description of the study area is provided in Section 2, before the key materials and underlying methods for this research are introduced in Section 3. A detailed description of the results is given in Section 4 while the paper concludes with the discussion of the findings and summary of concluding remarks and future research recommendations.

2. Study Area

The Eastern Cape province is one of the nine provinces and the second largest province in South Africa after the Northern Cape, with an area of close to 169,000 km². The province is located on the south-eastern part of the country, bordering the Western Cape and Northern Cape provinces to the west and north-west, respectively. The Eastern Cape province also borders the Free State province and Lesotho towards the north, KwaZulu-Natal province towards the north-eastern region and the Indian Ocean to the south-eastern and south regions, see Figure 1. The Eastern Cape's coastal areas are characterized by subtropical climatic conditions which predominate in KwaZulu-Natal and the Mediterranean climate of the Western Cape. Long, hot summers and moderate winters are mostly experienced in the Karoo towards the west, while the Great Escarpment towards Lesotho and the Free State experience snow in winter. Rainfall in the province exhibits bimodal patterns, with a winter rainfall (or all year rainfall) zone in the west, and summer rainfall zone in the east. On average, the Eastern Cape Province rainfall varies between 100 mm and 520 mm per year. Varying rainfall seasons result in varying growing periods, e.g., the summer seasonality advocates for the 4-Carbon (C4) grass production in the north, east and along the coastal belt, dominating with cattle and sheep production, whereas, the 3-Carbon (C3) grasses and shrubs predominate in the semi-arid central and western regions, favoring sheep and goat production.

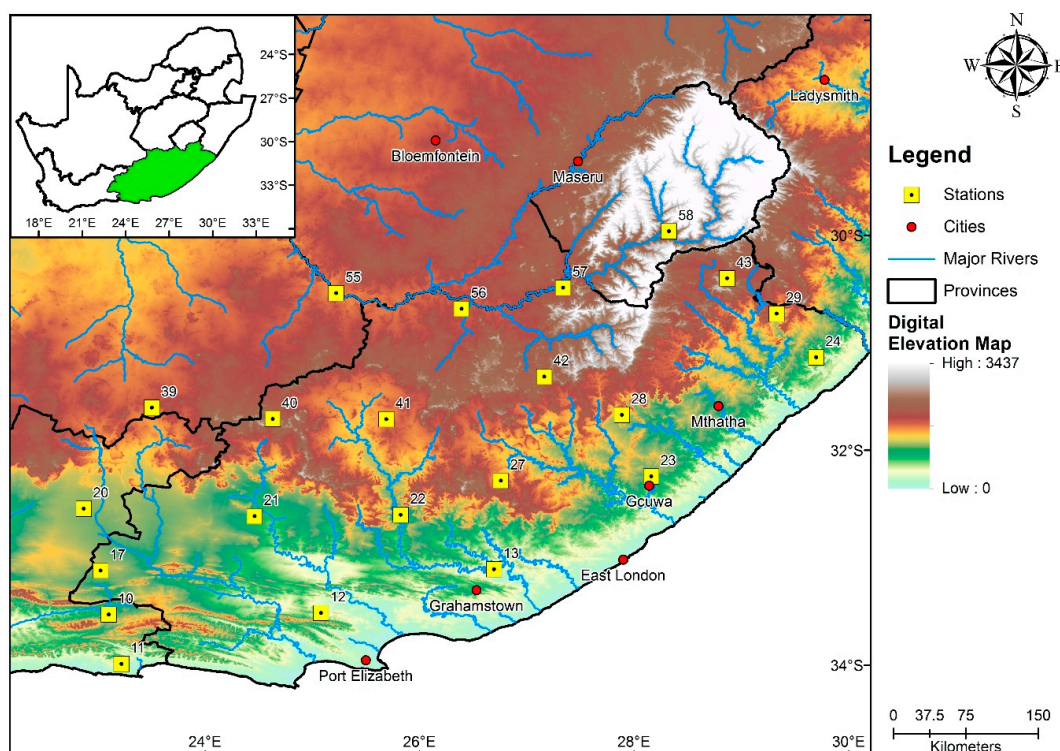


Figure 1. Eastern Cape province with the distribution of selected South African Weather Service climate district centroids and other areal characteristics.

In recent years, the Eastern Cape has experienced a severe drought, accompanied by negative socio-economic impacts across the province, with empirical evidence in Port Elizabeth, Graaff-Reinet, and Makhanda towns, where communities experienced severe water shortages and food security. Despite the persistence of these conditions and the inherent impacts, drought characteristics in the region have been understudied for years, with limitations being attributed to the complex influences of weather systems (manifested from the midlatitudes and tropics), the proximity of the region to the Agulhas Currents, as well as the strong topographic gradients.

3. Materials and Methods

3.1. Materials

Data analyzed in the current study was based on the monthly district rainfall from 1968 to 2018. A total of 22 rainfall climate districts distributed within the Eastern Cape province were selected and considered. These districts form part of the 94 rainfall climate districts, which cover the whole country, as delineated by the South African Weather Service (SAWS), formally known as the South African Weather Bureau 1972 (e.g., SAWB 1972). In general, these districts contain long-term monthly rainfall totals, from 1921 to present. The SAWS is responsible for updating the 94 rainfall districts and the process is performed monthly for detailed information on these rainfall climate districts the reader is referred to [38].

3.2. Methods

3.2.1. Drought Definition and Characterization Using the Standardized Precipitation Index

The SPI was developed with the basic understanding that a deficit in precipitation has cross-cut impacts on various types of water resources at different timescales, for example, ranging from soil moisture on a relatively short timescale and groundwater, reservoir storage, and streamflow,

at long-term scale. Designed to quantify deficit of precipitation at various timescales, the SPI can be used as a monitoring tool for all the three types of drought, namely meteorological, agricultural, and hydrological. Computation of SPI requires precipitation as the solely hydrological input. The procedural approach described in [9] was followed in this study to calculate the SPI time series at 6 and 12 accumulation periods. In this case, the monthly precipitation series for each station were fitted to a gamma probability density function defined as per Equation (1),

$$g(x) = \frac{1}{\beta^\alpha \Gamma(\alpha)} x^{\alpha-1} e^{-x/\beta} \quad (1)$$

where $\alpha > 0$ represents the shape parameter, $\beta > 0$ is a scalar parameter, $x > 0$ corresponds to the amount of precipitation and $\Gamma(\alpha)$ is the gamma function defined as,

$$\Gamma(\alpha) = \int_0^{\infty} y^{\alpha-1} e^{-y} dy \quad (2)$$

where α and β parameters of the gamma distribution are based on the approximation of [39], as given in Equations (3) and (4)

$$\alpha = \frac{1}{4A} \left(1 + \sqrt{1 + \frac{4A}{3}} \right) \quad (3)$$

$$\beta = \frac{\bar{x}}{\alpha}, \text{ with } A = \ln(\bar{x}) - \frac{\sum \ln(x)}{n} \quad (4)$$

where n is the number of observations. Integrating Equation (1) with respect to x leads to the computation of the cumulative probability function of the gamma distribution, expressed as in Equation (5),

$$G(x) = \int_0^x g(x) dx = \int_0^x \frac{1}{\beta^\alpha \Gamma(\alpha)} x^{\alpha-1} e^{-x/\beta} dx = \frac{1}{\Gamma(a)} \int_0^x t^{a-1} e^{-t} dt \quad (5)$$

Transforming Equation (5) into the standard normal distribution yields to the SPI, a time series representing both positive (for wet conditions) and negative (for dry conditions) values.

In order to characterize drought, we have used the run theory proposed by [40,41]. For this study, we have considered the drought duration and severity as two main drought characteristics derived using the algorithm summarized as follows:

- (a) Define drought events/episodes as periods when the SPI values (SPI-6/-12) are negative (inclusive of zero) as reported in [42].
- (b) Define drought epoch (DE) as the period when SPI values (SPI-6/-12) are consecutively zero and negative for six months. If during the six months, one month with positive SPI values occurs between the second and fourth month, the epochs before and after this intermittent occurrence of positive SPI value are combined to form a DE.
- (c) Drought duration (DD) is computed as the length of DE defined in (b), while drought severity (DS) is then computed as the integral of the SPI curve during the DE.

3.2.2. Multivariate Drought Analysis Using the Copulas

In this study, the copula method was used to assess the relationship between DD and DS, calculated from the SPI-6 and SPI-12 time series. To model the joint probability distribution of drought

characteristics (duration and severity), it was assumed that for $H(x,y)$, a joint distribution function, there exists a function expressed as in Equation (6),

$$H(x, y) = C(F_X(x), F_Y(y)) \tag{6}$$

In Equation (6), C is the copula, and $F_X(x)$ and $F_Y(y)$ are the marginal distributions, thus the cumulative distribution functions of X and Y , respectively. Suppose $U = F_X(x)$ and $V = F_Y(y)$, and given that X and Y are the marginal distributions, then the copula C can be defined as

$$C(u, v) = F(F_X^{-1}(u), F_Y^{-1}(v))$$

This allows the copula to be constructed as given by Equation (7).

$$C(F_X(x), F_Y(y)) = F(F_X^{-1}(F_X(x)), F_Y^{-1}(F_Y(y))) = H(x, y) \tag{7}$$

The marginal distributions for drought duration and severity were first identified, prior to the modelling of the joint probability distribution. This was achieved by fitting a number of probability distribution functions and assessing the best marginal distribution for the two drought features. The best fitted marginal distribution was identified based on the Akaike’s information criteria (AIC) and Bayesian information criteria (BIC).

The tail dependency structure of drought duration and severity was assessed based on the Multivariate Copula Analysis Toolbox (MvCAT) reported by [43]. A total of 10 copula distribution families were assessed, these are summarized in Table 1. After assessing the ranked scatter plot of drought characteristics, five copulas were selected for further analysis to identify the best copula. The correlation relationship between the drought characteristics was assessed by use of Kendall’s tau and Spearman’s correlation coefficients. Additionally, the best copula was identified based on the corresponding root mean square error (RMSE) and sorted based on the maximum likelihood. The best distribution function for the drought duration and severity was evaluated based on the best marginal distributions as well as the best.

Table 1. Summary of selected copula families adopted from [43]. The BB1 copula is derived from the combination of extreme cases of the Clayton and Gumbel copulas while BB5 is a 2-parameter extension of the Gumbel copula.

Name	Mathematical Description	Parameter Range	References
Gaussian	$\int_{-\infty}^{\Phi^{-1}(u)} \int_{-\infty}^{\Phi^{-1}(v)} \frac{1}{2\pi\sqrt{1-\theta^2}} \exp\left(\frac{2\theta xy - x^2 - y^2}{2(1-\theta^2)}\right) dx dy$	$\theta \in [-1, 1]$	[44]
Clayton	$\max(u^{-\theta} + v^{-\theta} - 1, 0)^{-1/\theta}$	$\theta \in [-1, \infty) \setminus 0$	[45]
Frank	$-\frac{1}{\theta} \ln \left[1 + \frac{(\exp(-\theta u) - 1)(\exp(-\theta v) - 1)}{\exp(-\theta) - 1} \right]$	$\theta \in \mathbb{R} \setminus 0$	[44]
Gumbel	$\exp\left\{-\left[(-\ln(u))^\theta + (-\ln(v))^\theta\right]^{1/\theta}\right\}$	$\theta \in [1, \infty)$	[44]
Joe	$1 - \left[(1-u)^\theta + (1-v)^\theta - (1-u)^\theta (1-v)^\theta \right]^{1/\theta}$	$\theta \in [-1, \infty)$	[44]
Galambos	$uv \left[\exp\left\{(-\ln(u))^{-\theta} + (-\ln(v))^{-\theta}\right\}^{-1/\theta}\right]$	$\theta \in [0, \infty]$	[46]
Cubic	$uv[1 + \theta(u-1)(v-1)(2u-1)(2v-1)]$	$\theta \in [-1, 2]$	[47]
BB1	$\left\{ 1 + \left[(u^{-\theta_1} - 1)^{\theta_2} + (v^{-\theta_1} - 1)^{\theta_2} \right]^{1/\theta_2} \right\}^{-1/\theta_1}$	$\theta_1 \in (0, \infty), \theta_2 \in (1, \infty)$	[48]
BB5	$\exp\left\{-\left[(-\ln(u))^{\theta_1} + (-\ln(v))^{\theta_1} - \left((- \ln(u))^{-\theta_1\theta_2} + (-\ln(v))^{-\theta_1\theta_2}\right)^{-1/\theta_2}\right]^{1/\theta_1}\right\}$	$\theta_1 \in [1, \infty), \theta_2 \in (0, \infty)$	[48]
Tawn	$\exp\left\{\ln(u^{1-\theta_1}) + \ln(v^{1-\theta_2}) - \left[(-\theta_1 \ln(u))^{\theta_3} + (-\theta_2 \ln(v))^{\theta_3}\right]^{1/\theta_3}\right\}$	$\theta_1, \theta_2 \in [0, 1], \theta_3 \in [1, \infty)$	[46]

3.2.3. Risk Analysis Framework-Based Return Periods

The copula-based method was used to calculate the joint return periods for the considered drought characteristics. The following equations were used to calculate the joint drought return periods,

$$T_{DS} = \frac{E(I_d)}{P(D \geq d \text{ or } S \geq s)} = \frac{E(I_d)}{1 - F_{DS}(d, s)} = \frac{E(I_d)}{1 - C(F_D(d), F_S(s))} \tag{8}$$

$$T'_{DS} = \frac{E(I_d)}{P(D \geq d \text{ and } S \geq s)} = \frac{E(I_d)}{1 - F_D(d) - F_S(s)} = \frac{E(I_d)}{1 - F_D(d) - F_S(s) + C(F_D(d), F_S(s))} \tag{9}$$

where $F_D(d)$ and $F_S(s)$ are cumulative marginal distribution functions of drought duration and severity, respectively; $E(I_d)$ is the expected time of inter-arrival time of drought events; and T_{DS} and T'_{DS} are the joint return periods of drought duration and severity (see [49] for further details).

For drought risks analysis, the annual return periods, T in years, (and the corresponding non-exceedance probability, q , see Equation (10)) were used. The multivariate drought risk analysis framework considers the duo drought variables: duration and severity thereby resulting to two forms of return periods akin to two non-exceedances commonly denoted as $T_{q;coop}$ and $T_{q;dual}$ as given in Equations (11) and (12), respectively. In essence, Equation (11) implies that both drought indices cooperate or collaborate as parts or as a whole, while Equation (12) signifies that both drought indices are conjunctive or work together.

$$T = \frac{1}{1 - q} \tag{10}$$

$$T_{q;coop} = \frac{1}{1 - C(q, q; \Theta)} = \frac{1}{\hat{C}^*(1 - q, 1 - q; \Theta)} \equiv \frac{1}{\text{cooperative risk}} \tag{11}$$

where $C(q, q; \Theta)$ and $\hat{C}^*(q', q'; \Theta)$ are the copula and the co-copula for the exceedance probability

$$q' = 1 - q,$$

respectively, that can be used to calculate the real return period of failure.

$$T_{q;dual} = \frac{1}{1 - \tilde{C}(q, q; \Theta)} = \frac{1}{\bar{C}(q, q; \Theta)} = \frac{1}{\hat{C}(q', q'; \Theta)} \equiv \frac{1}{\text{complement of dual protection}} \tag{12}$$

In Equation (12), $\tilde{C}(q, q; \Theta)$, $\bar{C}(q, q; \Theta)$ and $\hat{C}(q', q'; \Theta)$ are the dual of a copula function, the joint survival function and survival copula, respectively.

4. Results

4.1. Drought Characteristics

The top panel of Figure 2 depicts SPI-6 and SPI-12 time series for the selected climatic rainfall districts in the north-western part of the Eastern Cape province. Both SPI-6 and SPI-12 values show profound decadal drought variations. The two indices are ideally suited to describe the inherent total rainy seasons as well as the long-term drought conditions. Under the SPI-6 accumulation period, the three rainfall districts are characterized by, as reported in [13], levels 2 and 3 drought which is moderate-to-severe drought categories, thus ranging between $-1.50 < SPI \leq -1.00$ and $-2.00 < SPI \leq -1.50$, respectively. On the other hand, the SPI-12 depicts considerable decadal variability, wherein category 3 and 4 drought characteristics i.e., severe-to-extreme drought ($SPI \leq -2.00$), respectively. According to [16], such drought categories are likely to occur two to four times per century.

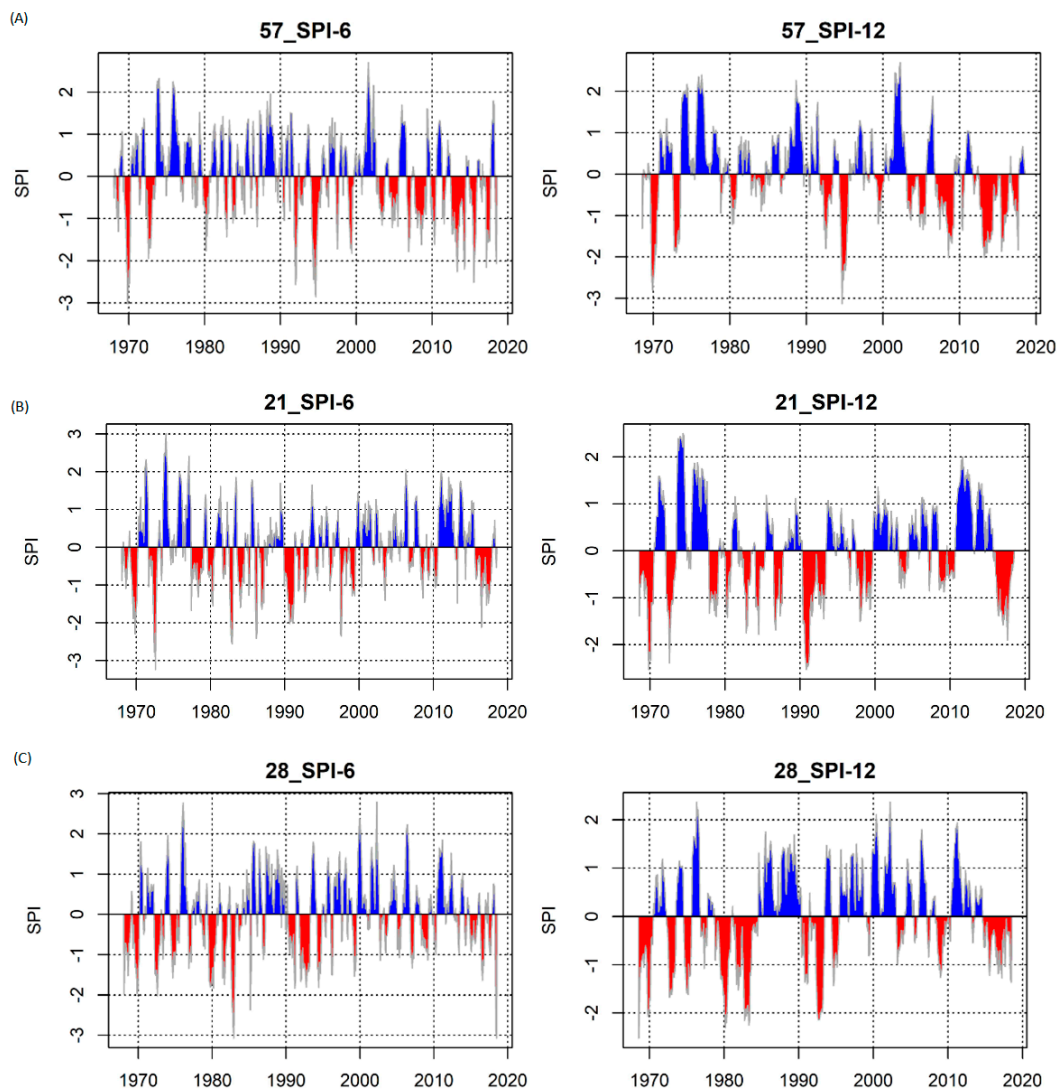


Figure 2. Standardized Precipitation Index (SPI) time series for selected climatic rainfall districts in (A) north-western, (B) south, and (C) south-eastern regions of the Eastern Cape province. Left panel: SPI-6 and right panel: SPI-12. The blue and red colors represent wet and dry epochs, respectively.

The south-eastern part of the study area (see for example middle and bottom panels) experienced more frequent and intense drought in the considered study period. In this regard, the SPI-12 in particular, illustrated an increase in the frequency of drought events at the respective rainfall districts. Most of the drought occurrences in these rainfall districts were characterized by the level 4 drought category (e.g., $SPI \leq -2.00$). Some of the drought occurrences between 1980/81 and 1990/91 were due to El Nino, a condition that brings very dry conditions along the south and south-eastern part of South Africa [50,51]. In general, the results demonstrate that the south and south-eastern parts of Eastern Cape are prone to prolonged and frequent drought episodes. These results corroborate with a weekly report by the Department of Water and Sanitation (DWS; 31 January 2019) which stated that the Makhanda dam level, formerly referred to as Grahamstown was at a critical (approaching day zero) level. A decrease of 1.4% was observed with a major drop from 57.4% to 56.0%. This has led to the intervention of the national DWS to partner with the Makhanda local municipality to preclude a total disaster.

In the current study, drought conditions were also assessed in terms of spatial distribution at 6- and 12-month time steps. In this regard, the derived results on the contrasts of drought episodes for SPI-6 and SPI-12 are depicted in Figure 3. The pie charts in Figure 3 are the numerical proportions of counts of drought episodes derived from SPI-6 and SPI-12 time series over the entire study period. It is evident from the figure that the percentage of drought episodes identified using SPI-6 was greater than those identified based on SPI-12 (by 16.5%). Furthermore, results show that the study area exhibits mean value of the drought episode of 6/4 during the entire study period, as computed from SPI-(6/-12)-month accumulation periods respectively. It was also determined that less than six drought episodes (computed from SPI-6) had a more likelihood of occurring (with a probability of ~0.8) while more than four drought episodes (derived from SPI-12) were more likely to occur (with a probability of ~0.6) in the study area. Figure 4 depicts maximal/extreme drought periods based on SPI-6 and SPI-12 experienced during the considered study period. As given in Figure 4, the study area experienced maximal drought periods that lasted for as little as 7/13 months extending to 33/48 months (for SPI-6/12). The average maxima drought period was determined to be approximately 1.5 and 2.2 years based on the SPI-6 and -12-accumulation periods, respectively. Overall, the results illustrate that the study area was more likely (with a probability of ~0.88) to experience maximal drought conditions that last more than 12 months, while drought conditions lasting over 24 months had a 33% likelihood of occurrence.

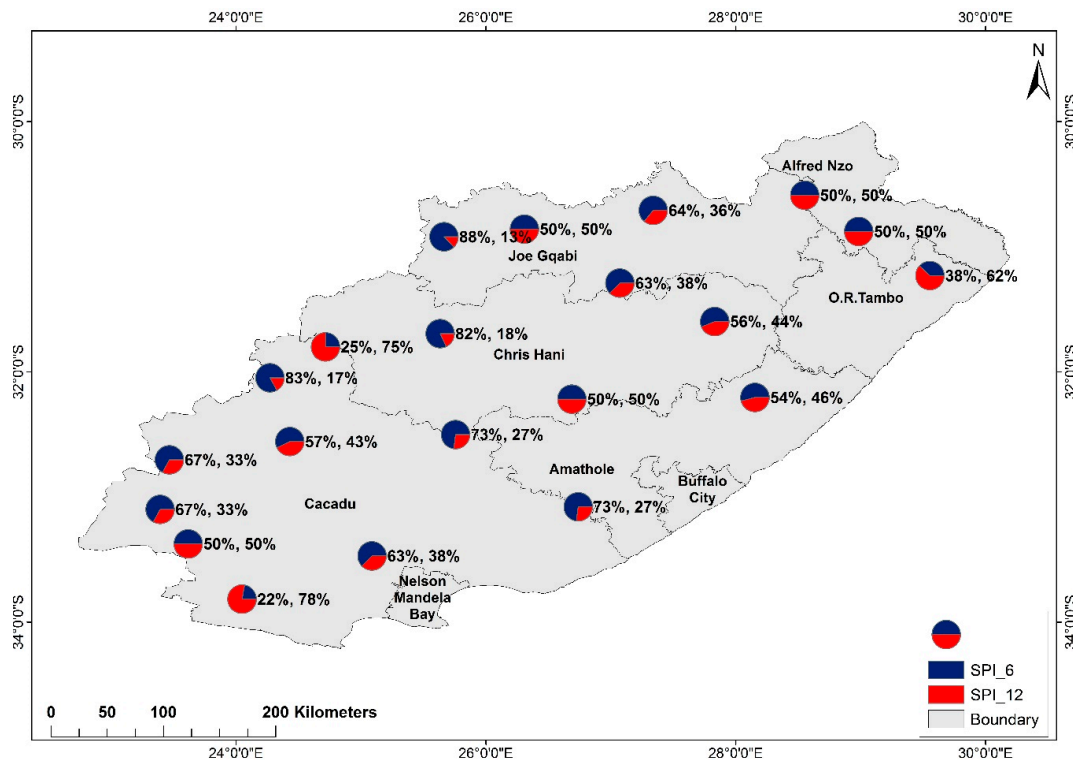


Figure 3. Proportion of occurrence of SPI-6 and SPI-12 drought episodes recorded across the Eastern Cape province, South Africa.

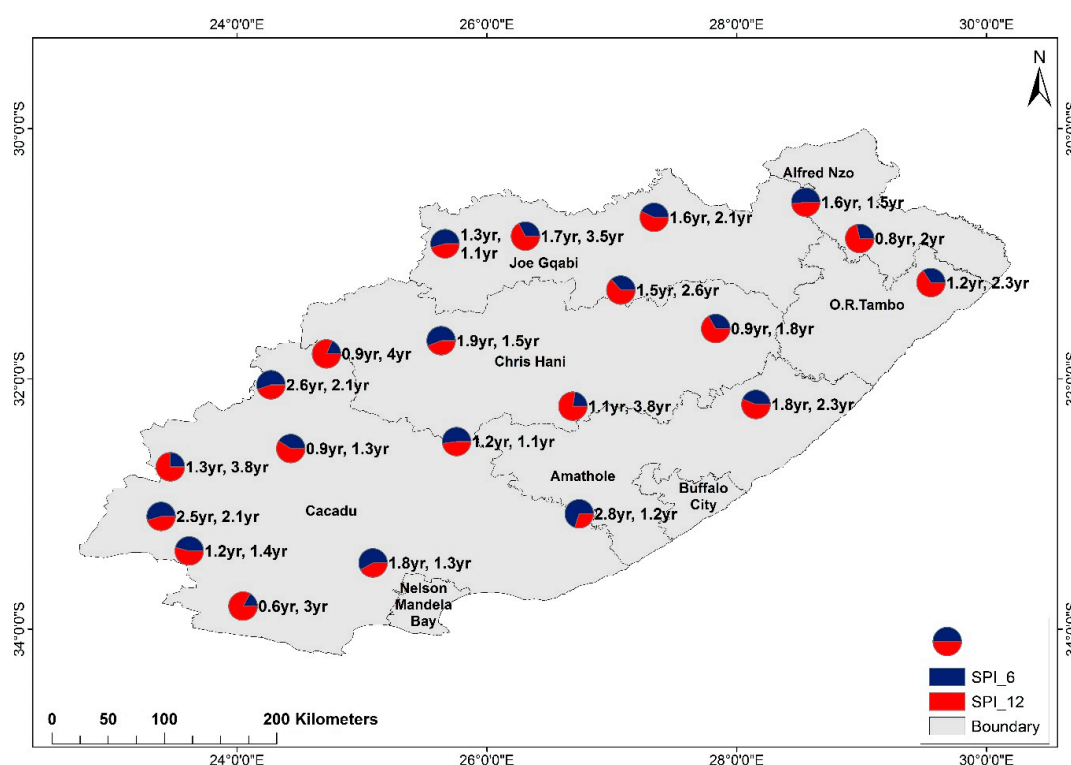


Figure 4. Spatial contrasts of maximal drought duration (in years) across the Eastern Cape province.

4.2. Characteristics of Marginal Distributions

Tables 2 and 3 give a summary of best marginal distributions fits to drought duration and severity computed from SPI-6 and SPI-12, across the selected rainfall districts, respectively. The correlation coefficient was based on Kendall's tau and Spearman tests and these are given in columns 4 and 5, of each table. Based on Table 2 (with regard to SPI-6), the generalized pareto and gamma distributions dominate across the region, providing the best distribution fit for drought duration to approximately 28% of the study area. In addition, the generalized pareto fits well to drought severity to approximately 23% of the study area, followed by Rayleigh, inverse Gaussian, and Weibull, each providing best fit to about 14% of the study area. The Spearman's correlation coefficient was higher across the region as compared to Kendall's tau. The coefficient values ranged between 0.4 to 0.8 for the Spearman's test and 0.3 to 0.6 for Kendall's tau. The calculated p -values (not shown) were statistically significant at 5% level across all the stations.

Based on Table 3 (for SPI-12), the generalized pareto distribution provides the best fit for both drought duration and severity across the selected rainfall districts. This distribution fits well to the drought duration and severity, covering 73% and 45% of the study area, respectively. Most of the rainfall districts depict a strong correlation between the drought duration and severity, as indicated from Spearman's coefficient values. These values ranged (correlations) between 0.2 and 0.7 for Kendall's tau and 0.2 to 0.8 for Spearman's test. The p -values were statistically significant across all but two rainfall districts.

Table 2. Best probability distributions in modelling marginal drought duration and severity computed from Standardized Precipitation Index (SPI)-6 time series.

District No.	Fitted Distribution		Correlation Coefficient		Significant at 5%?
	Duration	Severity	Kendall Rank	Spearman's Rank-Order	
10	Generalized Pareto	Rayleigh	0.566	0.745	Yes
11	Weibull	Generalized Pareto	0.563	0.743	-do- ¹
12	Generalized Pareto	Rayleigh	0.514	0.667	-do-
13	Logistic	Loglogistic	0.381	0.489	-do-
17	Rician	Rayleigh	0.525	0.707	-do-
20	Weibull	Generalized Pareto	0.394	0.539	-do-
21	Nakagami	-do-	0.540	0.706	-do-
22	Loglogistic	Inverse Gaussian	0.524	0.678	-do-
23	Generalized Pareto	Nakagami	0.509	0.668	-do-
24	Gamma	Weibull	0.278	0.364	-do-
27	Generalized Pareto	Birnbaumsaunders	0.570	0.734	-do-
28	Normal	Logistic	0.539	0.688	-do-
29	-do-	-do-	0.539	0.688	-do-
39	Generalized Pareto	Weibull	0.418	0.532	-do-
40	Birnbaumsaunders	Gamma	0.499	0.640	-do-
41	Gamma	Birnbaumsaunders	0.510	0.653	-do-
42	Birnbaumsaunders	Inverse Gaussian	0.558	0.718	-do-
43	Rician	Generalized Pareto	0.351	0.463	-do-
55	Loglogistic	Inverse Gaussian	0.519	0.643	-do-
56	Gamma	Generalized Pareto	0.498	0.645	-do-
57	Generalized Pareto	Weibull	0.602	0.737	-do-
58	Gamma	Nakagami	0.441	0.587	-do-

¹ -do-: denotes "as above".

Table 3. Best probability distributions in modelling marginal drought duration and severity computed from SPI-12 time series.

District No.	Fitted Distribution		Correlation Coefficient		Significant at 5%?
	Duration	Severity	Kendall Rank	Spearman's Rank	
10	Generalized Pareto	Rayleigh	0.512	0.661	Yes
11	-do-	Generalized Pareto	0.671	0.813	-do-
12	-do-	-do-	0.674	0.831	-do-
13	-do-	-do-	0.606	0.770	-do-
17	-do-	-do-	0.581	0.759	-do-
20	-do-	Birnbaumsaunders	0.442	0.577	-do-
21	-do-	Inverse Gaussian	0.576	0.736	-do-
22	-do-	Generalized Pareto	0.551	0.704	-do-
23	Rician	-do-	0.473	0.629	-do-
24	Generalized Pareto	Gamma	0.151	0.199	No
27	-do-	-do-	0.151	0.199	-do-
28	-do-	Generalized Pareto	0.634	0.782	Yes
29	Loglogistic	Weibull	0.418	0.542	-do-

Table 3. Cont.

District No.	Fitted Distribution		Correlation Coefficient		Significant at 5%?
	Duration	Severity	Kendall Rank	Spearman's Rank	
39	Generalized Pareto	Generalized Pareto	0.539	0.685	-do-
40	-do-	Gamma	0.507	0.693	-do-
41	-do-	Rayleigh	0.492	0.644	-do-
42	Rician	Nakagami	0.627	0.783	-do-
43	Gamma	Generalized Pareto	0.403	0.500	-do-
55	Weibull	-do-	0.652	0.801	-do-
56	Generalized Pareto	Gamma	0.495	0.635	-do-
57	-do-	Extreme value	0.619	0.790	-do-
58	Rician	Inverse Gaussian	0.334	0.409	-do-

4.3. Copula Joint Probability Distributions

Of the 10 copula families analyzed, five copulas were found to be suitable and therefore selected for the assessment of joint drought characteristics, thus the joint drought duration and severity features. A further analysis led to the selection of two copulas for the analysis of joint drought characteristics, see results presented in Table 4. The selection of the two copulas was based on assessing the RMSE values across the copulas and the rainfall districts. The RMSE values were ranked and based on max likelihood, the copulas were sorted from the least RMSE value to the highest value. The selected copulas are a combination of single, two and three parameters, with the computed values depicted in the tables. The best copula for each rainfall district is indicated in red, and this is Tawn copula for both SPI-6 and SPI-12 drought duration and severity features, followed by BB1 for SPI-6 and Joe for SPI-12. The Tawn copula had three parameters, whereas Joe and BB1 contained one and two parameters, respectively, see the estimated values in Table 4. The fact that Tawn copula predominates in both cases suggests that the three-parameter copulas were more suitable to assess the dependency of drought duration and severity.

Figures 5 and 6 depict plots of dependence structure between drought duration and severity represented at different probability space levels at a selected SAWS climate district. These were constructed from the best marginal distributions and best copula (e.g., Tawn and BB1 for SPI-6 and Tawn and Joe for SPI-12). In both cases, there is a tendency of asymmetric and skewness dependence structure of the drought features. There exist slight differences in the isolines produced by Tawn and BB1 copulas for SPI-6, and Tawn and Joe copulas for SPI-12, particularly between the 10th and 20th percentiles. Such differences could be attributed to tail dependence of the copulas, e.g., the Tawn copula has no tail dependence whereas BB1 and Joe have tail dependence coefficients. Nevertheless, the probability isolines derived from all the copulas are notably skewed to the left, suggesting a low probability of drought duration and high probability of drought severity.

Table 4. Selected copula joint probability distributions and their characteristics. Red indicates best copula for the climatic rainfall district. The RMSE denotes the Root Mean Square Error.

Rainfall Dist. No.	SPI-6				SPI-12			
	Tawn		BB1		Tawn		Joe	
	RMSE	θ_1	RMSE	θ_1	RMSE	θ_1	RMSE	θ_1
10	0.252	0.883	0.214	2.282	0.301	0.999	0.298	4.821
11	0.329	0.759	0.288	3.255	0.331	0.671	0.356	4.390
12	0.273	0.773	0.278	0.207	0.291	0.997	0.280	6.620

Table 4. Cont.

Rainfall Dist. No.	SPI-6				SPI-12			
	Tawn		BB1		Tawn		Joe	
	RMSE	θ_1	RMSE	θ_1	RMSE	θ_1	RMSE	θ_1
13	0.375	0.758	0.381	0.213	0.515	0.942	0.498	6.228
17	0.298	0.761	0.313	0.056	0.331	0.997	0.325	13.730
20	0.374	0.779	0.352	3.473	0.399	0.746	0.398	5.287
21	0.358	1.000	0.348	9.936	0.377	0.998	0.358	7.129
22	0.438	0.834	0.450	0.000	0.287	0.772	0.295	5.008
23	0.343	0.816	0.350	0.010	0.324	0.766	0.359	6.752
24	0.393	0.486	0.476	0.006	0.817	0.486	0.832	2.688
27	0.676	0.991	0.675	0.000	0.817	0.505	0.832	2.680
28	0.345	0.862	0.354	0.000	0.360	0.919	0.360	9.953
29	0.345	0.863	0.354	0.000	0.449	0.787	0.458	6.559
39	0.697	0.719	0.715	0.000	0.628	0.994	0.626	17.762
40	0.364	0.903	0.366	3.433	0.420	0.956	0.385	0.000
41	0.321	0.802	0.321	0.263	0.341	0.879	0.334	3.296
42	0.331	0.906	0.332	0.000	0.309	0.805	0.323	5.926
43	0.386	0.763	0.376	1.759	0.386	0.871	0.410	6.529
55	0.308	0.826	0.323	0.018	0.261	0.999	0.269	26.656
56	0.313	0.818	0.310	0.908	0.273	0.843	0.300	4.126
57	0.306	0.849	0.297	2.982	0.407	0.852	0.422	11.982
58	0.356	0.712	0.352	1.786	0.293	0.686	0.327	4.791

4.4. Risk Assessment Based on the Joint Drought Return Periods

Given that drought is a multivariate event, it is, therefore, best to fully account the inherent risks using a combination of two or more drought monitoring indicators. In the present study, the drought risks were assessed using the joint return periods derived from the Joe (and Gaussian, not shown) copula functions. In this case, the copula functions were calculated from the marginal distributions fitted by the two drought monitoring indicators i.e., drought duration and severity e.g., the SPI-6. The spatial distribution of joint return periods for the dual and cooperative cases (see Equations (10) and (11)) alongside the 2-, 5-, 10-, 20- and 100-year univariate return period are given in Figures 7 and 8, respectively. As depicted in Figure 7, the multivariate return period for the dual case was always longer across all the selected univariate return periods manifesting an overestimate of the drought risks. The dual (conjunctive) case contrasts cooperative multivariate case as shown in Figure 8, a consequence of the formulations given in Equations (10) and (11). In terms of drought risk analysis, the study area exhibited a noticeable north-west to south-east gradient with Buffalo City, Tambo and Alfred Zoo regions determined to have higher/lower risks in terms of the conjunctive/cooperative multivariate drought risk (copula) probability index.

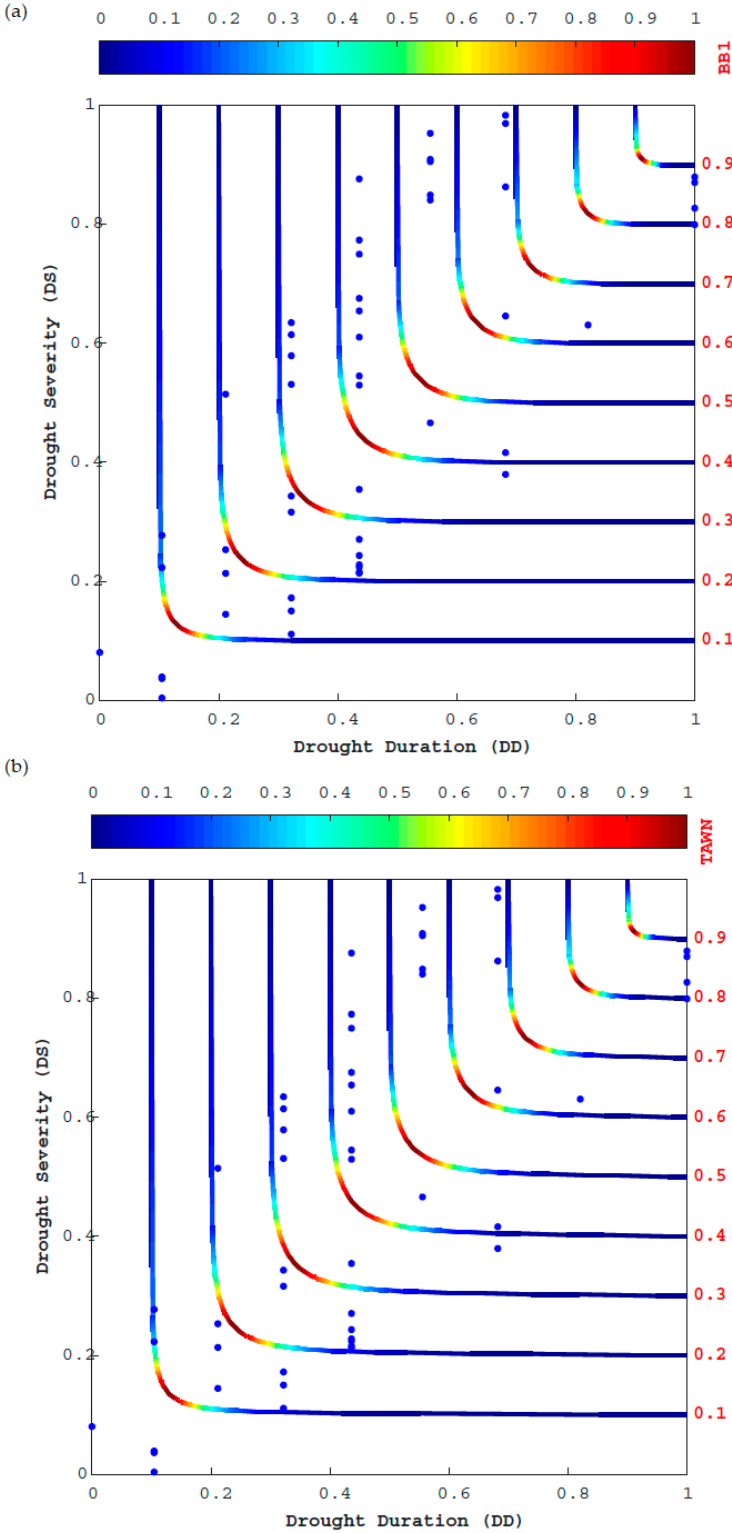


Figure 5. A typical dependence structure of drought duration and severity based on SPI-6 time series. In the figure (a) corresponds to BB1 and (b) corresponds to Tawn copulas.

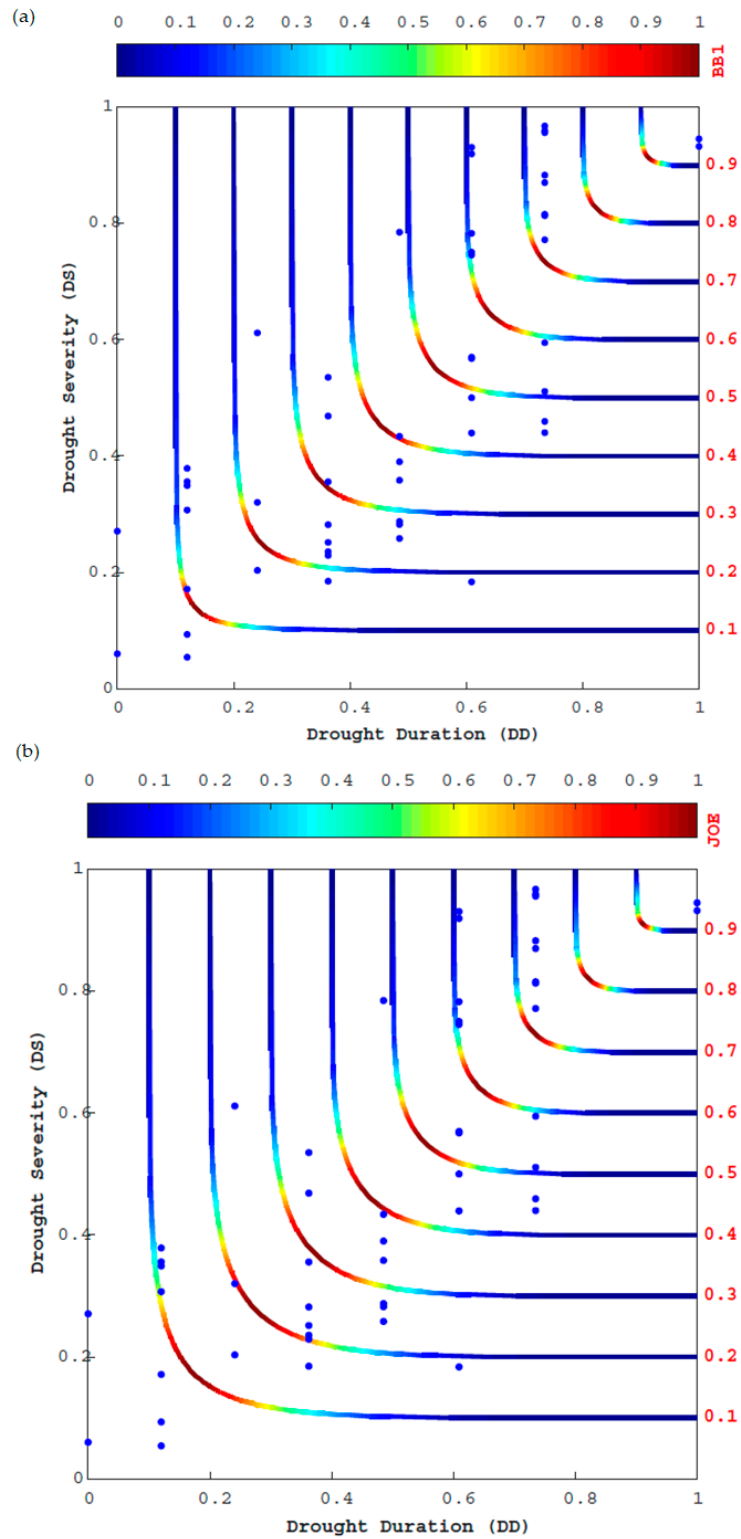


Figure 6. A dependence structure of drought duration and severity based on SPI-12 time series. In the figure, (a) corresponds to BB1 and (b) corresponds to Joe copulas.

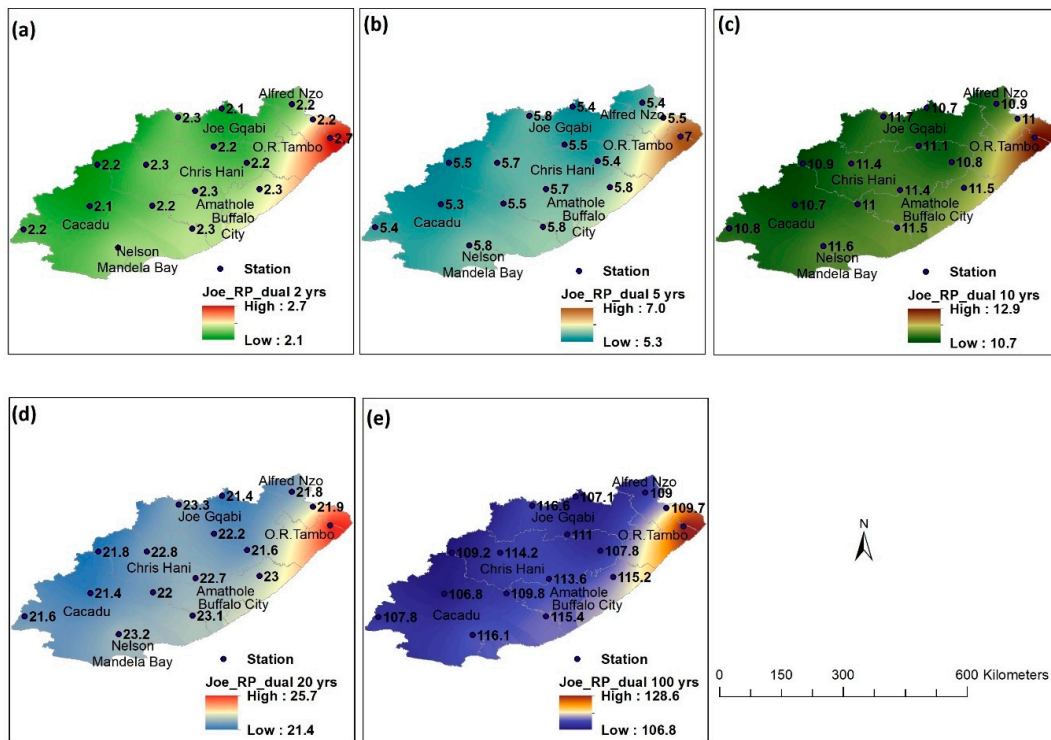


Figure 7. Spatial distribution of conjunctive return period corresponding to (a) 2-year, (b) 5-year, (c) 10-year, (d) 20-year, and (e) 100-year univariate risks of return periods based on the Joe Copula.

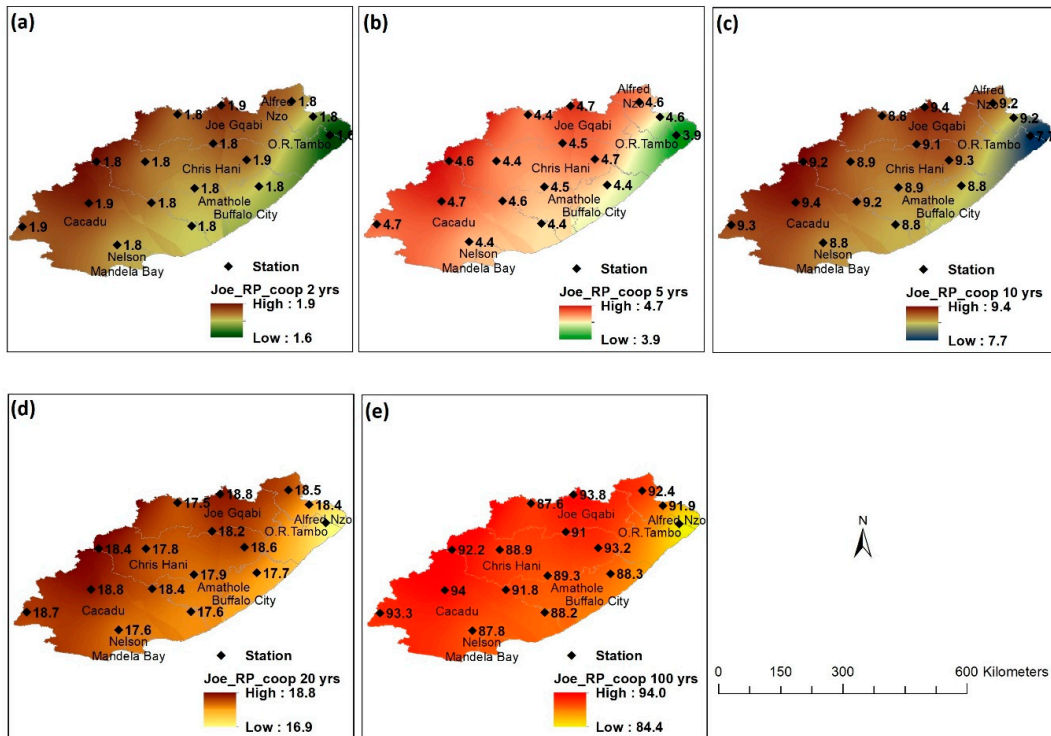


Figure 8. Spatial distribution of cooperative return period corresponding to (a) 2-year, (b) 5-year, (c) 10-year, (d) 20-year, and (e) 100-year univariate risks of return periods based on the Joe Copula.

5. Discussion and Conclusions

South Africa is generally known to be a water-stressed country because the available water resources do not meet the ever-increasing demand for e.g., domestic, industrial, and agricultural use. This situation is often exacerbated by the prolonged drought conditions albeit the intermittent flooding episodes. For instance, between 2014 and 2019, South Africa experienced persistent drought conditions which led to the declaration of drought as a national disaster (in March 2018) and many cities across the country such as Cape Town (Western Cape province), Port Elizabeth (Eastern Cape province), and Phalaborwa (Limpopo province) nearly approached “day-zero” state.

Studies, such as the current one, are therefore invaluable for drought monitoring, drought risk assessment, preparedness, and mitigation with applications in water resource management. It is for this purpose that, the present study has been undertaken to characterize drought conditions across the Eastern Cape province based on a multivariate risk assessment framework using a combination of drought duration and drought severity indicators. The literature on drought analysis over South Africa is generally abundant, a comprehensive assessment of drought risks at provincial scale and from the viewpoint of the drought risk probability index [52,53] across South Africa remains in-exhaustive and yet nascent. The present analysis results point to the following conclusions;

- (a) Five to eight drought episodes (with an average of 60–80% likelihood of occurrence) were experienced in the study area over the last five decades.
- (b) The Eastern Cape province is more likely to experience maxima drought conditions that last more than 12 months while drought conditions lasting over 24 months have a 33% likelihood of occurrence.
- (c) Five copulas families, from the Archimedean and Elliptical families, are duly suited to represent the multivariate characteristics of drought conditions in the study area. The spatial signature of the return periods from the five copulas was found to be comparable. These copula families are therefore ideal for drought risk quantification in the study area.
- (d) The conjunctive/cooperative multivariate drought risk (copula) probability index results illustrate that the area exhibits a noticeable north-west to south-east gradient with Buffalo City, Tambo and Alfred Zoo regions determined to have higher/lower risks.

This study, therefore, provides an invaluable, robust, and representative copula framework for a holistic drought risk analysis at provincial scale. It is therefore recommended that the methodology be extended for drought analysis across different provinces of South Africa and the southern African region, in support for drought preparedness, monitoring, and prediction.

Author Contributions: C.M.B. conceptualized, crafted the original draft, and finalized the manuscript. J.O.B. conceptualized, undertook the data analysis, discussed the results, and edited and approved the manuscript. J.P.d.W. prepared the study area map and edited the manuscript. A.M.A. generated the maps, contributed towards the discussion of the results, and edited the manuscript. N.N.Z. contributed towards the discussion of the results and edited the manuscript. K.P.N. discussed the results and edited the manuscript. All authors have read and agreed to the published version of the manuscript.

Funding: This research was supported by funding received from the Water Research Commission, South Africa and for this, the authors are grateful.

Acknowledgments: The authors wish to thank the three anonymous reviewers for providing extensive comments and suggestions that lead to the improvement of the manuscript quality.

Conflicts of Interest: The authors declare no conflict of interest.

References

1. Glickman, T.S. *Glossary of Meteorology*; American Meteorological Society: Boston, MA, USA, 2000; p. 855.
2. Pereira, L.S.; Cordery, I.; Iacovides, I. Coping with water scarcity. In *Addressing the Challenges*; Springer Science and Business Media: Dordrecht, The Netherlands, 2009; p. 382.

3. Wilhite, D.A.; Glantz, M.H. Understanding the drought phenomenon: The role of definitions. *Water Int.* **1985**, *10*, 111–120. [[CrossRef](#)]
4. Vicente-Serrano, S.M.; Begueria, S.; Eklundh, L.; Gimeno, G.; Weston, D.; Kenawy, A.E.; Lopez-Moreno, J.I.; Nieto, R.; Ayenew, T.; Konte, D.; et al. Challenges for drought mitigation in Africa: The potential use of geospatial data and drought information systems. *Appl. Geogr.* **2012**, *34*, 471–486. [[CrossRef](#)]
5. Wilhite, D.A.; Svoboda, M.D.; Hayes, M.J. Understanding the complex impacts of drought: A key to enhancing drought mitigation and preparedness. *Water Resour. Manag.* **2007**, *21*, 763–774. [[CrossRef](#)]
6. Ahmadalipour, A.; Moradkhani, H. Multi-dimensional assessment of drought vulnerability in Africa: 1960–2100. *Sci. Total Environ.* **2018**, *644*, 520–535. [[CrossRef](#)] [[PubMed](#)]
7. Zhang, Q.; Yu, H.Q.; Sun, P.; Singh, V.P.; Shi, P.J. Multisource data based agricultural drought monitoring and agricultural loss in China. *Glob. Planet. Chang.* **2019**, *172*, 298–306. [[CrossRef](#)]
8. Wilhite, D.A. Drought as a Natural Hazard: Concepts and Definitions (Chapter 1, pp. 3–18). In *Drought: A Global Assessment (Volume 1)*; Wilhite, D.A., Ed.; Routledge Publishers: London, UK, 2000.
9. McKee, T.B.; Doesken, N.J.; Kleist, J. The relationship of drought frequency and duration to time scales. In Proceedings of the Preprints, 8th Conference on Applied Climatology, Anaheim, CA, USA, 17–22 January 1993; pp. 179–184.
10. Vicente-Serrano, S.M.; López-Moreno, J.; Beguería, S.; Lorenzo-Lacruz, J.; Azorin-Molina, C.; Morán-Tejeda, E. Accurate computation of a streamflow drought index. *J. Hydrol. Eng.* **2012**, *17*, 318–332. [[CrossRef](#)]
11. Vicente-Serrano, S.M.; Begueria, S.; Lopez-Moreno, J.I. A multiscale drought index sensitive to global warming: The standardized precipitation evapotranspiration index. *J. Clim.* **2010**, *23*, 1696–1718. [[CrossRef](#)]
12. Palmer, W.C. *Meteorological Drought*; Research Paper No. 45; U.S. Department of Commerce Weather Bureau: Washington, DC, USA, 1965.
13. Botai, C.M.; Botai, J.O.; Dlamini, L.; Zwane, N.; Phaduli, E. Characteristics of Droughts in South Africa: A Case Study of Free State and North West Provinces. *Water* **2016**, *8*, 439. [[CrossRef](#)]
14. Botai, C.M.; Botai, J.O.; de Wit, J.C.; Ncongwane, K.P.; Adeola, A.M. Drought characteristics over the Western Cape Province, South Africa. *Water* **2017**, *9*, 876. [[CrossRef](#)]
15. Botai, C.M.; Botai, J.O.; Adeola, A.M. Spatial distribution of temporal precipitation contrasts in South Africa. *S. Afr. J. Sci.* **2018**, *114*. [[CrossRef](#)]
16. Rouault, M.; Richard, Y. Intensity and spatial extent of drought in southern Africa. *Geophys. Res. Lett.* **2005**, *32*, 1–4. [[CrossRef](#)]
17. Mondol, M.A.; Das, S.C.; Islam, M.N. Application of standardized precipitation index to assess meteorological drought in Bangladesh. *J. Disaster Risk Stud.* **2016**, *8*, 280. [[CrossRef](#)] [[PubMed](#)]
18. Mondol, M.A.; Ara, I.; Das, S.C. Meteorological Drought Index Mapping in Bangladesh Using Standardized Precipitation Index during 1981–2010. In *Advances in Meteorology*; Hindawi Publishing Corporation: Cairo, Egypt, 2017.
19. Malakiya, A.D.; Suryanarayana, T.M.V. Assessment of Drought Using Standardized Precipitation Index (SPI) and Reconnaissance Drought Index (RDI): A Case Study of Amreli. *IJSR* **2016**, *5*, 1995–2002.
20. Zhou, H.; Liu, Y. SPI Based Meteorological Drought Assessment over a Humid Basin: Effects of Processing Schemes. *Water* **2016**, *8*, 373. [[CrossRef](#)]
21. Miah, M.G.; Abdullah, H.M.; Jeong, C. Exploring standardized precipitation evapotranspiration index for drought assessment in Bangladesh. *Environ. Monit. Assess.* **2017**, *189*, 547. [[CrossRef](#)] [[PubMed](#)]
22. Tirivarombo, S.; Osupile, D.; Eliasson, P. Drought monitoring and analysis: Standardised Precipitation Evapotranspiration Index (SPEI) and Standardised Precipitation Index (SPI). *Phys. Chem. Earth* **2018**, *106*, 1–10. [[CrossRef](#)]
23. Archer, E.; Landman, W.; Malherbe, J.; Tadross, M.; Pretorius, S. South Africa’s winter rainfall region drought: A region in transition? *Clim. Risk Manag.* **2019**, *25*, 100188. [[CrossRef](#)]
24. Mackellar, N.C.; Hewitson, B.C.; Tadross, M.A. Namaqualand’s climate: Recent historical changes and future scenarios. *J. Arid Environ.* **2007**, *70*, 604–614. [[CrossRef](#)]
25. Shongwe, M.; Van Oldenborgh, G.J.; Hurk, B.; De Boer, B.; Coelho, C.; Aalst, M. Projected Changes in Mean and Extreme Precipitation in Africa under Global Warming. Part I: Southern Africa. *J. Clim.* **2009**, *22*. [[CrossRef](#)]
26. Du Plessis, J.A.; Schloms, B. An investigation into the evidence of seasonal rainfall patterns shifts in the Western Cape, South Africa. *J. S. Afr. Inst. Civ. Eng.* **2017**, *59*, 47–55. [[CrossRef](#)]

27. Shiau, J.T. Fitting drought duration and severity with two-dimensional copulas. *Water Resour. Manag.* **2006**, *20*, 795–815. [[CrossRef](#)]
28. Kao, S.C.; Govindaraju, R.S. A copula-based joint deficit index for droughts. *J. Hydrol.* **2010**, *380*, 121–134. [[CrossRef](#)]
29. Shiau, J.T.; Feng, S.; Nadarajah, S. Assessment of hydrological droughts for the Yellow River, China, using copulas. *Hydrol. Process.* **2007**, *21*, 2157–2163. [[CrossRef](#)]
30. Shiau, J.T.; Modarres, R. Copula-based drought severity-duration-frequency analysis in Iran. *Meteorol. Appl.* **2009**, *16*, 481–489. [[CrossRef](#)]
31. Wong, G.; Lambert, M.F.; Leonard, M.; Metcalfe, A.V. Drought analysis using trivariate copulas conditional on climate states. *J. Hydrol. Eng.* **2010**, *15*, 129–141. [[CrossRef](#)]
32. Madadgar, S.; Moradkhani, H. Drought analysis under climate change using copula. *J. Hydrol. Eng.* **2013**, *18*, 746–759. [[CrossRef](#)]
33. Lee, T.; Modarres, R.; Quarda, T. Data-based analysis of bivariate copula tail dependence for drought duration and severity. *Hydrol. Process.* **2013**, *27*, 1454–1463. [[CrossRef](#)]
34. Chen, L.; Singh, V.; Guo, S.; Mishra, A.; Guo, J. Drought Analysis Using Copulas. *J. Hydrol. Eng.* **2013**, *18*, 797–808. [[CrossRef](#)]
35. Hoffman, M.T.; Carrick, P.J.; Gillson, L.; West, A.G. Drought, climate change and vegetation response in the succulent karoo, South Africa. *S. Afr. J. Sci.* **2009**, *105*, 54–60. [[CrossRef](#)]
36. Adisa, O.M.; Botai, J.O.; Adeola, A.M.; Botai, C.M.; Hassen, A.; Darkey, D.; Tesfamariam, E.; Adisa, A.T.; Adisa, A.F. Analysis of drought conditions over major maize producing provinces of South Africa. *J. Agric. Meteorol.* **2019**. [[CrossRef](#)]
37. Rouault, M.; Richard, Y. Intensity and spatial extension of drought in South Africa at different time scales. *Water SA* **2003**, *4*, 489–500. [[CrossRef](#)]
38. Kruger, A.C.; Nxumalo, M.P. Historical rainfall trends in South Africa: 1921–2015. *Water SA* **2017**, *43*, 285–297. [[CrossRef](#)]
39. Thom, H.C.S. A Note on the Gamma Distribution. *Mon. Weather Rev.* **1958**, *86*, 117–132. [[CrossRef](#)]
40. Yevjevich, V. *An Objective Approach to Definitions and Investigations of Continental Hydrologic Droughts*; Hydrology Paper 23; Colorado State University: Fort Collins, CO, USA, 1967; p. 18.
41. Mesbahzadeh, T.; Mirakbari, M.; Saravi, M.M.; Sardoo, F.S.; Miglietta, M.M. Meteorological drought analysis using copula theory and drought indicators under climate change scenarios (RCP). *Meteorol. Appl.* **2020**, *27*, e1856. [[CrossRef](#)]
42. McKee, T.B.; Doesken, N.J.; Kleist, J. Drought monitoring with multiple time scales. In Proceedings of the Ninth Conference on Applied Climatology, Dallas, TX, USA, 15–20 January 1995; pp. 233–236.
43. Sadegh, M.; Ragno, E.; AghaKouchak, A. Multivariate Copula Analysis Toolbox (MvCAT): Describing dependence and underlying uncertainty using a Bayesian framework. *Water Resour. Res.* **2017**, *53*, 5166–5183. [[CrossRef](#)]
44. Li, C.; Singh, V.P.; Mishra, A.K. A bivariate mixed distribution with a heavy-tailed component and its application to single-site daily rainfall simulation. *Water Resour. Res.* **2013**, *49*, 767–789. [[CrossRef](#)]
45. Clayton, D.G. A model for association in bivariate life tables and its application in epidemiological studies of familial tendency in chronic disease incidence. *Biometrika* **1978**, *65*, 141–151. [[CrossRef](#)]
46. Huynh, V.N.; Kreinovich, V.; Sriboonchitta, S. *Modeling Dependence in Econometrics*; Springer: New York, NY, USA, 1996.
47. Durrleman, V.; Nikeghbali, A.; Roncalli, T. A Note about the Conjecture on Spearman’s rho and Kendall’s tau. *SSRN Electron. J.* **2000**. [[CrossRef](#)]
48. Genest, C.; Favre, A.C. Everything you always wanted to know about copula modeling but were afraid to ask. *J. Hydrol. Eng.* **2007**, *12*, 347–368. [[CrossRef](#)]
49. Ekanayake, R.; Perera, K. Analysis of Drought Severity and Duration Using Copulas in Anuradhapura, Sri Lanka. *Br. J. Environ. Clim. Chang.* **2014**, *4*, 312–327. [[CrossRef](#)]
50. Mulenga, H.M.; Rouault, M.; Reason, C.J.C. Dry summers over north-eastern South Africa and associated circulation anomalies. *Clim. Res.* **2003**, *25*, 29–41. [[CrossRef](#)]
51. Reason, C.J.C.; Phaladi, R.F. Evolution of the 2002–2004 drought over northern South Africa and potential forcing mechanisms. *S. Afr. J. Sci.* **2005**, *101*, 544–552.

52. Rashid, M.M.; Beecham, S. Characterization of meteorological droughts across South Australia. *Meteorol. Appl.* **2019**. [[CrossRef](#)]
53. Wang, Y.; Zhang, Q.; Yao, Y. Drought vulnerability assessment for maize in the semiarid region of northwestern China. *Theor. Appl. Climatol.* **2020**, *140*, 1207–1220. [[CrossRef](#)]



© 2020 by the authors. Licensee MDPI, Basel, Switzerland. This article is an open access article distributed under the terms and conditions of the Creative Commons Attribution (CC BY) license (<http://creativecommons.org/licenses/by/4.0/>).